Int J Cardiovasc Imaging (2012) 28:1035–1047
DOI 10.1007/s10554-011-9932-0

ORIGINAL PAPER

Intuitive visualization and quantification of intraventricular convection in acute ischemic left ventricular failure during early diastole using color Doppler-based echocardiographic vector flow mapping

Jing Lu · Wenhua Li · Yu Zhong · Anguo Luo · Shenghua Xie · Lixue Yin

Received: 22 February 2011 / Accepted: 21 July 2011 / Published online: 4 August 2011

Abstract The aim of this study was to make an intuitive visualization of intraventricular convection (IC) and quantification of intraventricular convection velocity (ICV) in acute ischemic left ventricular (LV) failure of open-chest canines during early diastole contrast to the baseline conditions using color Doppler-based echocardiographic vector flow mapping (VFM). The animal care committee approved this prospective study. In 6 anesthetized open-chest beagle models, the emergence time and the emergence sites of IC in the LV cavity during early diastole were visualized at the standard apical 3-chamber (AP3c) views with the VFM at baseline conditions and after coronary artery ligation. The global ICV and the ICV at the basal, middle and apical levels of LV at the AP3c views at T1, T2, T3, T4, and T5 between both states were compared respectively (T1: the beginning of LV rapid filling period; T2: the middle of LV rapid filling period; T3: the peak of LV rapid filling period; T4: the middle of period of reduced filling; T5: the end of early diastole.). Acute ischemic LV failure with a marked increase in LV end diastolic volume and LV minimal diastolic pressure was induced by coronary artery ligation. The IC appeared only during the period of reduced filling at baseline conditions, and limited to the basal level of LV cavity. But the IC appeared throughout all the early diastole, and was seen almost occupying whole LV cavity during ischemia. The peak of the global ICV for both states appeared at T4. The global ICV at the AP3c views in acute ischemic failure LV cavity increased than those of baseline conditions at the T1 (6.593 ± 0.834 cm^2/s vs. 0.000 ± 0.000 cm^2/s, $P < 0.001$), T2 (9.457 ± 0.852 cm^2/s vs. 0.000 ± 0.000 cm^2/s, $P < 0.001$), T3 (14.765 ± 1.791 cm^2/s vs. 2.030 ± 0.502 cm^2/s, $P < 0.001$), T4 (25.392 ± 4.640 cm^2/s vs. 6.688 ± 1.343 cm^2/s, $P < 0.001$), and T5 (15.890 ± 3.159 cm^2/s vs. 2.518 ± 0.869 cm^2/s, $P < 0.001$). And the ICV at the basal, middle and apical levels at AP3c views in acute ischemic failure LV cavity also increased than those of baseline conditions at the same phase of early diastole ($P < 0.01$), except for the ICV at the LV basal level at T1. VFM is a powerful tool for visualization IC and quantification of ICV on profiles of LV flow fields, which can give intriguing insights into the subtle, flow-associated LV fluid dynamics of normal and abnormal cardiac function. It will be of great practical importance to elucidate the accurate physiological and the pathophysiological significance of the IC in further studies, so as to determine whether the cardiac function can be precisely evaluated with IC

J. Lu · W. Li · A. Luo · S. Xie · L. Yin (✉)
Department of Cardiovascular Ultrasound and Non-invasive Cardiology, Sichuan Academy of Medical Sciences and Sichuan Provincial People's Hospital, 2nd West Section, 1st Roundway, Chengdu, Sichuan 610072, China
e-mail: yinlixue@yahoo.com

Y. Zhong
Institute of Ultrasound Image, Chongqing Medical University, Chongqing, China

related index, and to incorporate VFM into clinical routine practice in the future.

Keywords Echocardiography · Vector flow mapping · Intraventricular convection · Ischemia · Heart failure

Abbreviations

VFM	Vector flow mapping
LV	Left ventricle/ventricular
IC	Intraventricular convection
ICV	Intraventricular convection velocity
T1	The beginning of LV rapid filling period
T2	The middle of LV rapid filling period
T3	The peak of LV rapid filling period
T4	The middle of period of reduced filling
T5	The end of early diastole
AP3c	Standard left ventricular apical 3-chamber
HR	Heart rate
LVEDV	Left ventricular end diastolic volume
LVESV	Left ventricular end systolic volume
LVSV	Left ventricular stroke volume
LVEF	Left ventricular ejection fraction
$LVSP_{max}$	Left ventricular maximal systolic pressure
$LVDP_{min}$	Left ventricular minimal diastolic pressure
dp/dt_{max}	The maximal upstroke velocity of left ventricular systolic pressure

Introduction

Cardiology is about flow [1]. The relationship between blood flow patterns and cardiovascular disease is important because disturbed flow may be both a consequence and a cause of disease [2]. Therefore, qualitative and quantitative assessment of the intracardiac flow field, especially the left ventricular (LV) flow patterns, has received extensive attention [3–5]. Color M-mode Doppler images acquired time delay between peak velocity at the mitral tip and the apical region was determined as an index of LV flow propagation that can reflect LV relaxation [6]. Studies proved that during early diastole, the increased time delay accompanied with dominated intraventricular convection (IC) within the acute ischemic failure LV [7, 8]. Although the abnormal IC in the dilated ischemic LV was observed and its potential clinical relevance was indicated about eleven years ago, there are only limited medical imaging techniques for visualization of IC and quantification of IC related index. Therefore, we hypothesize that quantification of IC related index in LV cavity with innovative tool has clinical relevance, which may provide preliminary support for developing of a new marker of heart healthy status.

Color Doppler-based echocardiographic vector flow mapping (VFM), which extracts potential information of real-time color Doppler flow images by using an algorithm of computational fluid mechanics, provides new insights for intuitive visualization and quantification of the LV flow field on a three-dimensional flow plane [9]. One potential important application of VFM was applied to quantify the flow volume of the LV vortex flow in a cut plane. The algorithm of VFM technology for depict the vortex profile based on bellow assumptions: (1) A vortex is bilaterally symmetric in shape and velocity profile, i.e. the influx of a vortex equal to its outflow volume in a scan plane; (2) The velocity components perpendicular to the scan plane in a vortex are zero. According to these special assumptions, the real three-dimensional flow structure of vortex can not be precisely assessed, but the algorithm actually facilitate intuitive visualization of IC and quantification of intraventricular convection velocity (ICV) on a flow fields profile with reasonable accurate [10].

It has not yet been established whether IC in LV cavity can be quantified with non-invasive imaging techniques. The aim of this study was to make an intuitive visualization of IC and quantification of ICV in acute ischemic LV failure of open-chest canines at the standard apical 3-chamber (AP3c) views during early diastole contrast to the baseline conditions using VFM.

Methods

Animal preparation

Six healthy beagles (3 male and 3 female; 9–16 kg, mean weight 12.40 ± 2.88 kg) were provided by Experimental Animal Institute of Sichuan Academy of Medical Sciences. All animals involved received

human care in compliance with accredited facilities of Chinese Association for Accreditation of Laboratory Animal Care. The studies and animal care protocols were reviewed and approved by the local Institutional Care and Animal Research Committee. Preoperative 12 h fasting was applied in all animals. Intramuscular injection of atropine 0.5 mg and aminazine 50 mg was used for sedation and thirty minutes later, ketamine 100 mg and fentanyl 100 mg were given intramuscularly for anesthesia. Anaesthetizd beagles were placed in a supine position. A polyvinyl cannula was inserted into the left femoral vein for drug and fluid administration. Slow intravenous infusion of saline maintained hydration throughout surgery, and anesthesia was maintained using continuous intravenous infusion of ketamine (500 mg/h) and fentanyl (500 mg/h). Mechanical ventilation was used via an orotracheal tube with 40–60% O_2, ventilation frequency: 20 bpm, tidal volume: 10–15 ml/kg/min (IE 902-C ventilator; Ruideyigeer Co, China). Supplemental doses of anesthetics were given throughout the experiment to suppress the medial ocular reflex. Arterial blood gases and pH were kept stable by adjusting ventilation or bicarbonate infusion. All the sheaths and catheters were washed and filled using heparin sodium solution before insertion. Under the monitoring of gray-scale echocardiography, a 7F Millar catheter tip was introduced into the LV outflow tract via left carotid artery, with electrocardiography monitoring (Lead 2000; Jingjiang Electronic Co, China). The heart was exposed by a lateral thoracotomy and suspended in a pericardial cradle. Left anterior descending coronary artery distal to the first diagonal branch was isolated and ligatured completely with 4# silk suture after baseline imaging collection had been completed.

Echocardiography

Commercially available ultrasonic equipment (Prosound α10; Aloka Co, Japan) with a 1.88–5.00 MHz phased array cardiac transducer (UST-52101) was used. The maximal velocity range of the color bar was preset from 50 to 63 cm/s, and the baseline of color bar was kept at 0 cm/s. The frame rate of real-time color Doppler flow imaging was maintained from 23 to 30 frames/s. To maintain flow data quality in the LV apex, sufficient coupling medium were added into the space between transducer and the epicardium during echocardiography. For all beagles, LV real-time two-dimensional gray-scale and color Doppler flow images of standard apical 3-chamber (AP3c) views in 3 consecutive cardiac cycles were acquired and stored into DICOM image format via trans-epicardial Doppler echocardiography at baseline and 30 min later of the left anterior descending coronary artery ligated completely.

Data collection

LV end diastolic volume (LVEDV), end systolic volume (LVESV), stroke volume (LVSV) and ejection fraction (LVEF) were derived via Simpson rule. LV maximal systolic pressure ($LVSP_{max}$) and minimal diastolic pressure ($LVDP_{min}$), and the maximal upstroke velocity of LV systolic pressure (dp/dt_{max}) were measured through pressure–time curves stored in electrophysiological equipment.

All stored dynamic color Doppler flow images were transferred into VFM workstation (DAS-RS1; Aloka Co, Japan) for off-line analysis. A simple line was placed across the mitral annulus to acquire the time-flow curve of LV inflow, and five informative points during the early diastolic period were determined (Fig. 1): The beginning of LV rapid filling period (T1), the middle of LV rapid filling period (T2), the peak of LV rapid filling period (T3), the middle of period of reduced filling (T4), and the end of early diastole (T5). Three sample lines were placed across the LV chamber at the levels of apex, papillary muscle and mitral valve tips paralleled each other and approximately perpendicular to the longitudinal axis of LV cavity at the AP3c views. Then the trans-lines velocity profile display was turned on for intuitive visualization of the emergence time and the emergence sites of the IC between the LV base and the LV apex (Fig. 2). To acquire the ICV at the basal, middle and apical level of LV cavity, normal velocity profile display was turned on. The positive trans-line flow volume (Q+) and the negative trans-line flow volume (Q−) at different levels were automatically displayed and recorded (Fig. 3, upper row). The ICV at each level on the AP3c cut planes was calculated according to the trans-line flow volume respectively: ICV = min (Q+, Q−). To quantify the global ICV on the AP3c cut planes, the vortex components display was turned on. The sum of the maximal flow volume of the LV vortices at the AP3c cut planes is equal to the global ICV on this three-dimensional flow profile at a special informative point during the early diastole (Fig. 3, lower row).

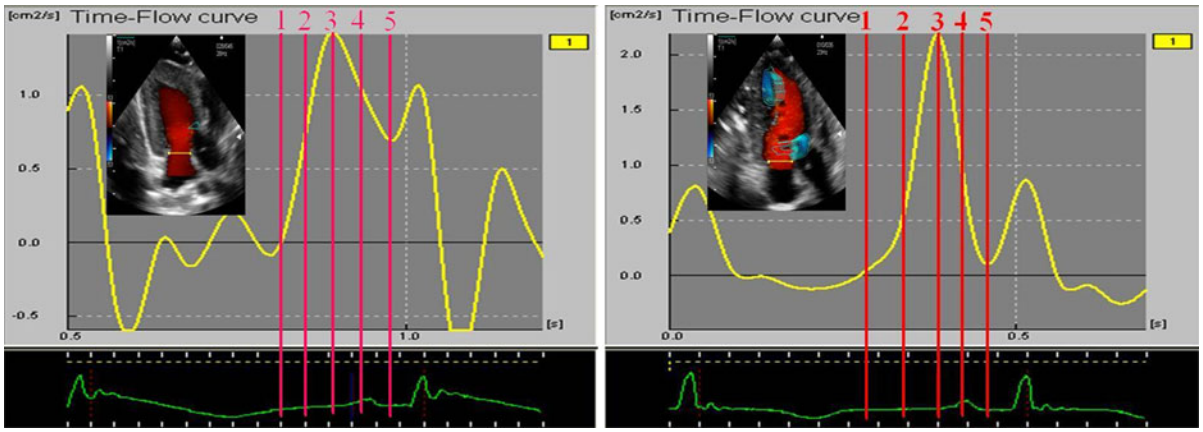

Fig. 1 Time-flow curves of beagles LV inflow at both states. *Left panel* was derived from the baseline condition, and the right from the acute ischemic state. The curves have 2 positive waves during the diastolic phase. The first one indicated the early diastole, the followed one indicated the atrial systole period. The five *red lines* numbered from 1 to 5 represent following five informative points during the early diastole respectively. At the beginning of LV rapid filling period (T1), at the middle of LV rapid filling period (T2), at the peak of LV rapid filling period (T3), at the middle of period of reduced filling (T4), and at the end of early diastole (T5)

Algorithm of VFM technology facilitates us to acquire ICV on a flow fields profile with reasonable accurate [9, 10]. A standard setting of an Aloka machine gives a color Doppler sector image at a special informative point comprising 80 beam lines in regular angle increments and 392 pitches in regular increments along each beam line, so there are 31,360 digital velocity data points in a single dataset at the AP3c cut plane. We placed three sample lines at the basal, middle and apical level of LV cavity perpendicular to the longitudinal axis of LV cavity at the AP3c views, and the digital velocity data points on each sample line were decomposed into normal velocity and parallel velocity. Normal velocity is the flow velocity component that perpendicular to the sample line. If the color Doppler velocity across the sample line has only positive or negative sign, we determined that no IC at this level. If the color Doppler velocity across the sample line has both positive and negative sign, we determined that IC appeared at this level. Then the ICV at each level was calculated according to the trans-line flow volume respectively: ICV = min (Q+, Q−). The direction of the ICV at each level is perpendicular to the sample line. To acquire the global ICV on the AP3c cut plane at each informative point, we drew assistance from the algorithm of VFM technology about vortex profile. Connection of every digital velocity data point at the same depth along the acoustic beams on a fanlike scan plane can construct an arc. During the vortex profile analysis, at each informative point on the AP3c cut planes is analyzed on an arc at each depth. The spatial resolution VFM is 5 × 5 mm, so the interval of the neighboring arcs is about 5 mm on the fanlike scan plane. If the color Doppler velocity profile on an arc has only positive or negative sign, the flow across the arc is considered to be non-vortical laminar flow. If it has both positive and negative sign, the flow across the arc is considered to be a combination of a single non-vortical laminar flow and several vortical laminar flows. The fraction with the opposite sign to the integration result is assumed to represent a half part of a vortex. Its counterpart should be included in the fraction with same sign as the integration result and is extracted in a rotationally symmetrical manner. Color Doppler data along each arc on the special cut plane were integrated to calculate the maximal 2D flow volume of each LV vortex at the special informative point. Therefore, the sum of the maximal flow volume of the LV vortices at the AP3c cut plane actually represented the global ICV on this three-dimensional flow profile. The direction of the global ICV on the AP3c cut planes is parallel to the acoustic beams.

Two double-blinded examiners repeatedly performed the VFM acquired ICV for intraobserver and interobserver analysis. The second observer repeated the measurements 2 weeks after the first time.

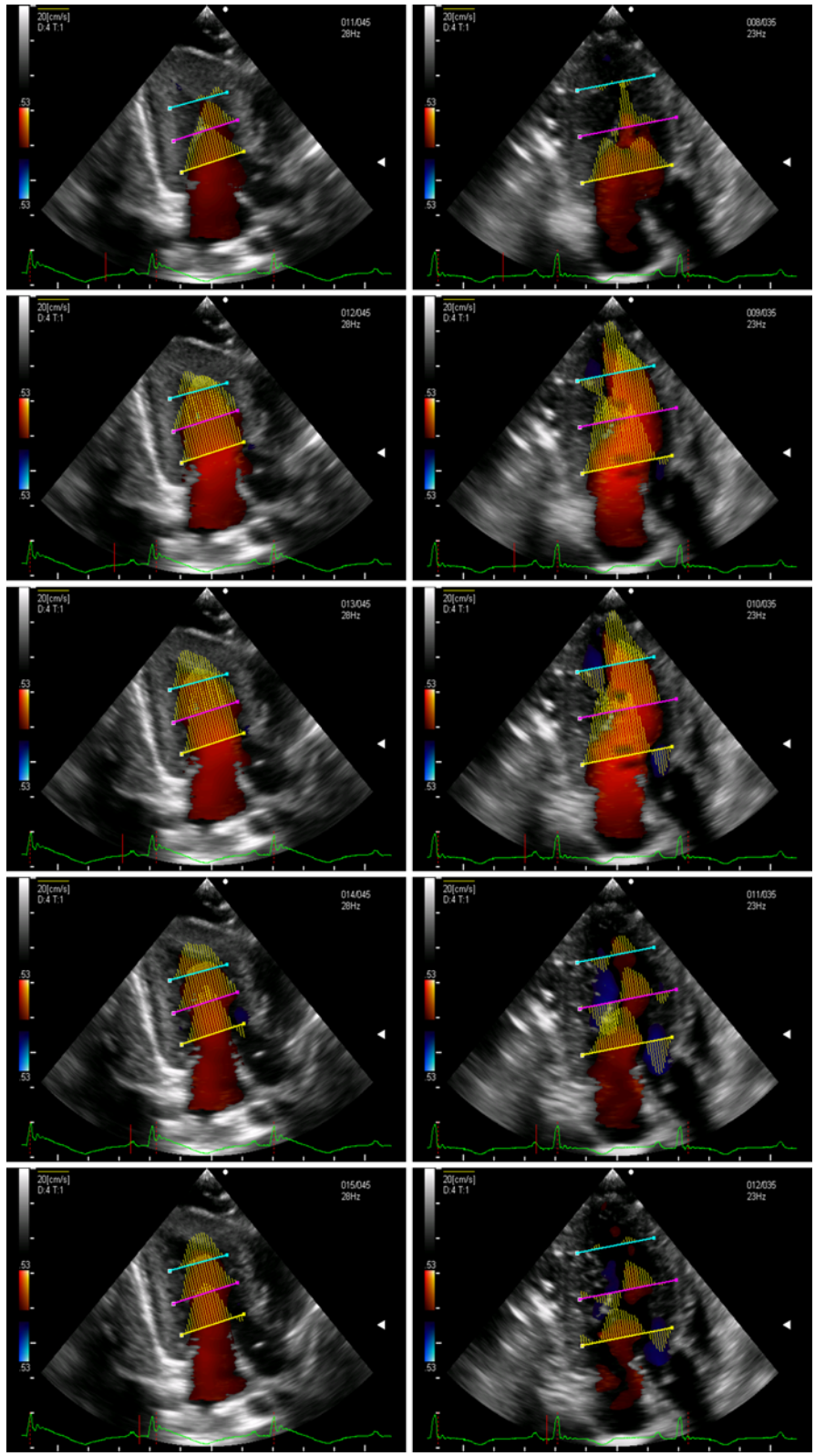

Fig. 2 Velocity profile displays of the IC within the beagles LV cavity. *Left panel* was derived from the baseline condition, and the *right* from the acute ischemic state. The 5 rows from the upper to the lower were derived from T1 to T5 respectively. Three sample lines were placed across the LV chamber at the levels of apex, papillary muscle and mitral valve tips at the AP3c views. The IC at the AP3c views appeared at T3, T4, and T5 at baseline conditions, and limited to the basal level of LV cavity. But the IC appeared earlier at the LV middle and apical levels at T1, and was seen at each level of the LV cavity from T2 to T5 during ischemia

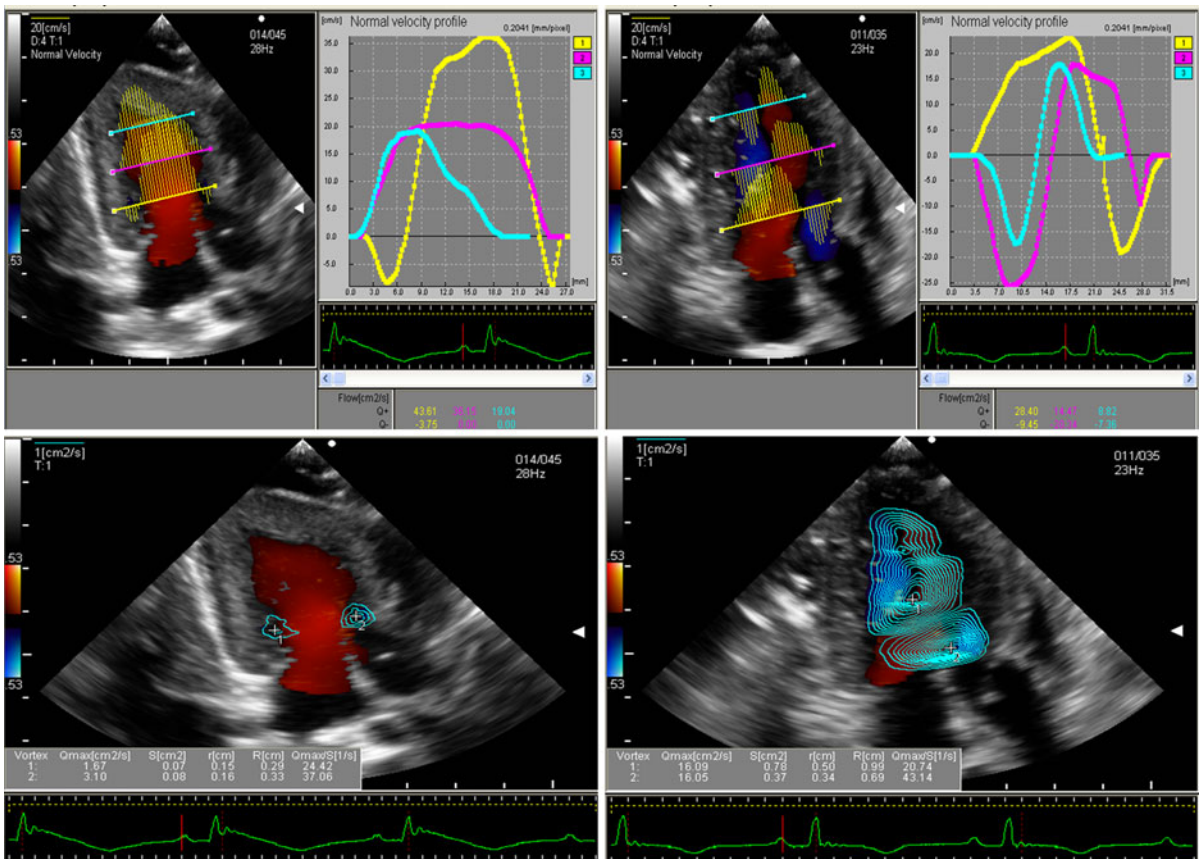

Fig. 3 Normal velocity profile display of the positive trans-line flow volume (Q+) and the negative trans-line flow volume (Q−) at the basal, middle and apical level of LV cavity (*upper row*). The ICV at each level on the special LV cut plane was calculated according to the trans-line flow volume respectively: ICV = min (Q+, Q−). *Left panel* in the *upper row* was derived from the baseline condition at T4, and the ICV at the LV basal, middle and apical level were 3.75 cm^2/s, 0 cm^2/s, and 0 cm^2/s respectively. *Right panel* in the *upper row* was derived from the acute ischemic state at T4, and the ICV at the LV basal, middle and apical level were 9.45 cm^2/s, 14.47 cm^2/s, and 7.36 cm^2/s, respectively. Vortex components display of the beagles LV flow fields at the AP3c cut planes (*lower row*). The LV vortex related parameters are displayed automatically in the lower part of the maps, and the first parameter Qmax is the maximal flow volume of the interrogated LV vortex. The sum of the Qmax of the LV vortices on the special LV cut plane is equal to the global ICV at this flow profile. *Left panel* in the *lower row* was derived from the baseline condition at T4, and the global ICV was 4.77 cm^2/s. *Right panel* in the *lower row* was derived from the acute ischemic state at T4, and the global ICV was 32.14 cm^2/s

Statistical analysis

Statistical tests were performed with SPSS 13.0 statistical software (SPSS, Chicago, IL, USA). Quantitative data are expressed as mean ± SD. We tested for data normalcy using the Shapiro–Wilk test. The global ICV and the ICV at the basal, middle and apical level of LV at the AP3c views at T1, T2, T3, T4, and T5 between both states were compared respectively using the paired Student *t* test. Also, the bias tests for intraobserver and interobserver agreement were compared using paired *t* test. Statistical significance was defined as $P < 0.05$. For *P* values <0.000, a value of <0.001 was chosen.

Results

Effect of acute myocardial ischemia on the LV structure and function

In all animals, the complete protocol was performed. Acute ischemic LV failure was induced by coronary artery ligation. We found statistical significance

Table 1 Comparisons of the LV function between both states

Variable	Baseline (n = 6)	Ischemia (n = 6)	*t* value	*P* value
HR (beat/min)	133.000 ± 7.014	124.833 ± 9.663	1.879	0.119
LVEDV (ml)	19.432 ± 2.311	25.335 ± 1.627	9.701	0.001
LVESV (ml)	8.582 ± 1.236	15.243 ± 1.479	11.217	0.001
LVSV (ml)	10.515 ± 0.926	10.092 ± 7.760	1.587	0.175
LVEF (%)	55.950 ± 1.798	39.899 ± 3.001	11.175	0.001
$LVSP_{max}$ (mmHg)	117.500 ± 15.630	89.000 ± 16.137	15.494	0.001
$LVDP_{min}$ (mmHg)	9.167 ± 2.317	14.667 ± 3.011	4.919	0.004
dp/dt_{max} (mmHg/s)	2082.833 ± 65.687	1375.974 ± 291.173	5.731	0.002

Results were expressed as mean ± SD with six data points collected in each analysis. The *t* values and the *P* values were given by comparing the results of the baseline with the acute ischemic state using paired Student's *t* test. Statistical significance was defined as $P < 0.05$. For *P* values <0.000, a value of <0.001 was chosen

HR heart rate, *LVEDV* left ventricular end diastolic volume, *LVESV* left ventricular end systolic volume, *LVSV* left ventricular stroke volume, *LVEF* left ventricular ejection fraction, $LVSP_{max}$ left ventricular maximum systolic peak pressure, $LVDP_{min}$ left ventricular minimum diastolic pressure, dp/dt_{max} the maximum upstroke velocity of left ventricular systolic pressure

existing in all parameters between both states except for the heart rate and the LVSV (Table 1). The LVEDV, the LVESV, and the $LVDP_{min}$ increased, and the LVEF, the $LVSP_{max}$, as well as the dp/dt_{max} decreased at the ischemic conditions.

Velocity maps at the AP3c views during early diastole

Velocity vectors reflect the blood flow patterns on a cut plane of LV flow fields. Circular arrangement of the vectors represents the profiles of vortex flow at the AP3c views. At baseline, the LV inflow was a pattern of column motion with no apparent vortex flow at T1 and T2. At T3, a small clockwise rotation vortex appeared under the anterior mitral leaflet. At T4 and T5, two vortices were seen curling back behind each mitral leaflet. During ischemia, a counterclockwise rotation vortex appeared earlier inside the LV apex at T1. Two contrarotation large size vortices were observed beside the LV inflow at each informative point from T2 to T5, the counterclockwise rotation vortex inside the lower part of ischemic failure LV cavity, and the clockwise rotation vortex near the anterior mitral leaflet (Fig. 4).

The emergence time and the emergence sites of IC in the LV cavity

The IC at the AP3c views appeared at T3, T4, and T5 at baseline conditions, and limited to the basal level of LV cavity. But the IC appeared earlier at the LV middle and apical levels at T1, and was seen at each level of the LV cavity from T2 to T5 during ischemia (Fig. 2).

The quantitative analysis of ICV at the AP3c views

During early diastole, the peak of the global ICV at the AP3c views appeared at T4 for both states (Fig. 5). The global ICV in acute ischemic failure LV cavity during early diastole increased than those of baseline conditions at the same phase of early diastole (Table 2).

The ICV on the AP3c cut plane at the basal, middle and apical level at AP3c views in the ischemic failure LV cavity increased than those of baseline conditions at the same phase of early diastole ($P < 0.001$), except for the ICV at LV basal level at T1 (Table 3).

Intraobserver and interobserver analysis

There was no statistically significant difference between the 2 observers or within an observer for the global ICV at the AP3c views (Table 4). And there was no statistically significant difference between the 2 observers or within an observer for the ICV at the basal, middle and apical level of LV cavity ($P > 0.05$).

Discussion

Convection is the relative motion of each part within fluid, and was classified into natural convection and

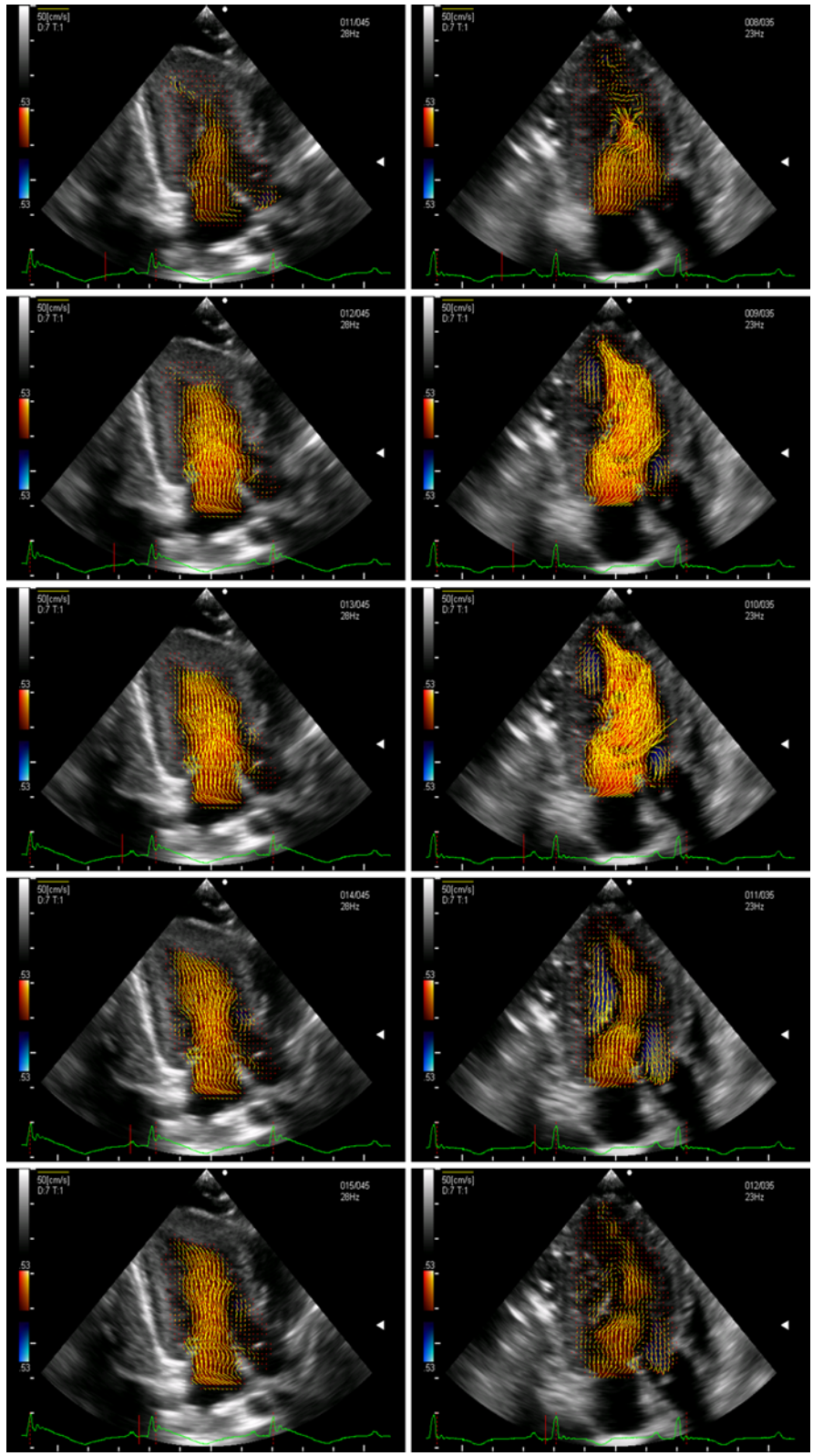

Fig. 4 Velocity maps of the beagles LV flow fields at the AP3c views during early diastole. Velocity vectors reflect the blood flow patterns on a cut plane of LV flow fields. *Circular* arrangement of the vectors represents the profiles of vortex flow. *Left panel* was derived from the baseline condition, and the right from the acute ischemic state. The 5 rows from the upper to the lower were derived from T1 to T5, respectively. At baseline, the LV inflow was a pattern of column motion with no apparent vortex flow at T1 and T2. At T3, a small clockwise rotation vortex appeared under the anterior mitral leaflet. At T4 and T5, two vortices were seen curling back behind each mitral leaflet. During ischemia, abnormal large size vortices with long persistence time appeared earlier inside the dilated ischemic LV cavity

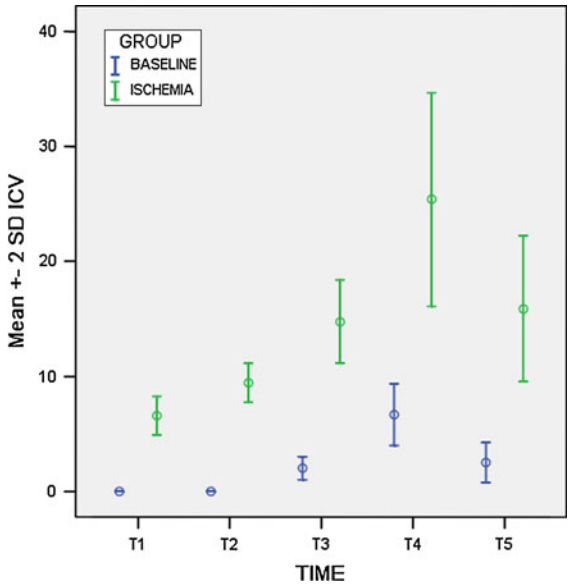

Fig. 5 The cluster error bar shows that the peak of the global ICV at the AP3c cut planes for both states appeared at T4, and the global ICV in acute ischemic LV cavity during early diastole increased than those of baseline conditions at the same phase of early diastole. T1 ~ T5 on the time axis represent the five informative points numbered from 1 to 5 respectively

Table 2 Comparisons of the global IVC (cm^2/s) on the AP3c cut planes between both states

Time	Baseline (n = 6)	Ischemia (n = 6)	*t* value	*P* value
T1	0.000 ± 0.000	6.593 ± 0.834	19.364	0.001
T2	0.000 ± 0.000	9.457 ± 0.852	27.197	0.001
T3	2.030 ± 0.502	14.765 ± 1.791	17.781	0.001
T4	6.688 ± 1.343	25.392 ± 4.640	11.802	0.001
T5	2.518 ± 0.869	15.890 ± 3.159	8.990	0.001

Results were expressed as mean ± SD with six data points collected in each analysis. The *t* values and the *P* values were given by comparing the results of the baseline with the acute ischemic state using paired Student's *t* test. Statistical significance was defined as $P < 0.05$. For *P* values <0.000, a value of <0.001 was chosen

T1 the beginning of LV rapid filling period, *T2* the middle of LV rapid filling period, *T3* the peak of LV rapid filling period, *T4* the middle of period of reduced filling, *T5* the end of early diastole

forced convention. The latter is one of the principal formative mechanisms of LV vortex flow. To say in other words, LV vortex is the pattern of the manifestation of the IC. Cardiac function could be measured more precisely through quantitative analysis of the LV vortex [11], but an extremely difficult issue to resolve when discussing flow vortices is to accurately assess their perimeter with conventional clinical imaging techniques. The phenomenon of IC within ischemic failure LV was observed by Steine et al., and its potential clinical relevance was indicated in their prominent study [8]. This result raised the possibility that the quantitative analysis of the IC related index within LV cavity may play an important role in evaluating the heart healthy status.

The IC and the LV vortices during early diastole at baseline conditions

With VFM, the substantial formations of the LV vortices under mitral valves during the period of reduced filling of early diastole at baseline conditions were observed, and the IC appeared limit to the basal level of LV cavity at the same phase. Ebbers et al. [12] also found that vortices can be seen around the mitral inflow in healthy LV during the period of reduced filling using time-resolved three-dimensional phase-contrast MRI. In order to interpret the phenomenon appropriately, it is most essential to understand the atrioventricular filling dynamics in healthy heart [12–15]. During the rapid filling period, the left intraventricular pressure gradient initiates by actively relaxation and enlargement of the LV, creating a pressure in the LV that is lower than in the left atrium. The pressure gradient draws blood from the atrium and accelerates the blood rush into the LV apex. Therefore, the inflow adopts a reasonably straight route towards the apex, without significant secondary flow at T1 and T2. Continuing inflow, caused by inertia and reentry of pressure wave, creates a reversal of the initial transmitral pressure difference. This results in moderately advanced deceleration and redirection of the LV filling blood flow during the period of reduced filling. From T3 to T5, the blood flow starts to change direction and vortices can be seen around the mitral inflow. At T5, i.e. the onset of atrial systole period, a pressure gradient arises caused by contraction the left atrium. This pressure field reaccelerates the inflow, which weakens the vortical pattern under mitral valves. The changes of atrioventricular pressure gradient during early diastole can explain our results that the peak of the global ICV appeared at T4. Why dose the vortices and IC under healthy conditions were seen limit to the basal level of LV cavity? This phenomenon may be ascribed to the

Table 3 Comparisons of ICV (cm^2/s) at the basal, middle and apical level of LV on the AP3c cut planes between both states

Level	Time	Baseline (n = 6)	Ischemia (n = 6)	*t* value	*P* value
Basal	T1	0.000 ± 0.000	0.000 ± 0.000	–	–
	T2	0.000 ± 0.000	2.288 ± 0.765	7.324	0.001
	T3	1.663 ± 0.546	3.692 ± 0.803	5.029	0.004
	T4	3.592 ± 0.331	8.577 ± 1.237	12.638	0.001
	T5	1.877 ± 0.496	4.727 ± 1.189	5.076	0.004
Middle	T1	0.000 ± 0.000	3.272 ± 0.800	10.013	0.001
	T2	0.000 ± 0.000	4.082 ± 0.961	10.401	0.001
	T3	0.000 ± 0.000	8.570 ± 1.592	13.190	0.001
	T4	0.000 ± 0.000	12.062 ± 2.631	11.231	0.001
	T5	0.000 ± 0.000	9.000 ± 1.692	13.030	0.001
Apical	T1	0.000 ± 0.000	1.975 ± 0.865	5.593	0.003
	T2	0.000 ± 0.000	3.428 ± 0.908	9.249	0.001
	T3	0.000 ± 0.000	4.432 ± 0.951	11.411	0.001
	T4	0.000 ± 0.000	6.960 ± 1.464	11.648	0.001
	T5	0.000 ± 0.000	4.423 ± 0.895	12.102	0.001

Results were expressed as mean ± SD with six data points collected in each analysis. The *t* values and the *P* values were given by comparing the results of the baseline with the acute ischemic state using paired Student's *t* test. Statistical significance was defined as $P < 0.05$. For *P* values <0.000, a value of <0.001 was chosen

The sign "–" represents that the *t* value and the *P* value cannot be given because the standard error of the difference is 0

T1 the beginning of LV rapid filling period, *T2* the middle of LV rapid filling period, *T3* the peak of LV rapid filling period, *T4* the middle of period of reduced filling, *T5* the end of early diastole

Table 4 Interobserver and Intraobserver Analysis of the global ICV (cm^2/s) on the AP3c cut planes

State	Time	Observer			*P* value
		1 (n = 6)	2-First (n = 6)	2-Second (n = 6)	
Baseline	T3	2.030 ± 0.502	1.997 ± 0.0.486	2.135 ± 0.571	>0.05
	T4	6.688 ± 1.343	6.066 ± 1.356	6.487 ± 1.455	>0.05
	T5	2.518 ± 0.869	2.213 ± 0.779	2.474 ± 0.587	>0.05
Ischemia	T1	6.593 ± 0.834	6.013 ± 0.834	6.587 ± 0.812	>0.05
	T2	9.457 ± 0.852	8.922 ± 0.778	9.356 ± 0.803	>0.05
	T3	14.765 ± 1.791	15.311 ± 1.256	14.875 ± 1.902	>0.05
	T4	25.392 ± 4.640	23.586 ± 4.571	24.381 ± 4.912	>0.05
	T5	15.890 ± 3.159	14.288 ± 2.995	16.012 ± 3.363	>0.05

Results were expressed as mean ± SD with six data points collected in each analysis. The *P* values were given by comparing the results of the baseline with the acute ischemic state using paired Student's *t* test

T1 the beginning of LV rapid filling period, *T2* the middle of LV rapid filling period, *T3* the peak of LV rapid filling period, *T4* the middle of period of reduced filling, *T5* the end of early diastole

Venturi effect. For example, fanlike airstream rush into leeside when wind blow over a wall. Here, the semi-closed mitral waves during the period of reduced filling just as the wall, and the space between the mitral waves and the LV basal wall just as the leeside. The VFM acquired evolutional characteristic of the LV vortices and the IC during early diastole under baseline conditions were corresponding to a perfect computational fluid dynamics study about the formative procedure of LV vortex ring during early diastole, which based on solid hemodynamic theory of LV filling [16].

Significant changes of IC and the LV vortices in the acute ischemic failure LV

Abnormal relaxation induced by cardiac ischemia or infarction has been described in animals and in patients, and the abnormal diastolic filling can be observed early in cardiac ischemia. Using contrast echocardiography, Beppu et al. proved the existence of recirculation flow in the dog LV during coronary ligation [17]. They found that the contrast echoes did not reach the apex but turned upward to the outflow tract in the middle of the dilated ischemic LV cavity during diastole. In an investigation in patients with dilated ischemic LV using magnetic resonance velocity vector mapping, the LV inflow was seen to be directed toward the free wall, giving rise to a well-developed circular flow pattern turning back toward the septum and the outflow tract that persists through the diastole [18]. Taylor et al. reported that complex blood flow vortex formation appeared near the infracted segments of the LV wall, which not identified in healthy ventricles [19]. Retardation of apical filling in acute ischemic failure reflecting slowing of LV relaxation was pointed out by Stugaard and colleagues [7]. Steine et al. confirmed in their further study that the slowing of flow propagation within the ischemic LV appeared to represent a shift in apical filling from a pattern of column motion to a pattern dominated by convection [8]. In addition, Delemarre et al. concluded from their prospective clinical study that LV spatial apical flow patterns could predict clinical course of the patients with acute myocardial infarction [20]. Aforesaid evidences indicated that abnormal LV vortex flow and enhanced IC must exist within the dilated ischemic LV cavity, and this phenomenon must have its potential clinical relevance. But both the quantification of IC and its pattern of manifestation, i.e. the quantification of LV vortex flow are long-standing and challenging tasks.

With the VFM, we found abnormal large size vortices with long persistence time appeared within the dilated ischemic LV cavity during early diastole, and the ICV increased at the same phase. These characteristics could be ascribed to the abnormal pressure fields within the dilated LV cavity, which result from cardiac ischemia. Regional differences in the rate of relaxation could contribute to the intraventricular pressure gradients [21]. Using the method of analyzing the LV inflow propagation velocity, Duval-Moulin et al. confirmed that during myocardial ischemia, the premature cessation of diastolic filling is associated with increased diastolic pressures due to the slowing of relaxation and reduction of chamber compliance, which may lead to compensatory elevation of LV filling pressure [22]. This investigation provides us powerful supports for understanding the premature appearance of the LV vortices and IC within the dilated ischemic LV at T1 and T2 in our study. The decreasing diastolic atrioventricular pressure gradient during early diastole resulting from this convective deceleration, termed "convective deceleration load", which adversely impacts diastolic inflow [22]. This adverse impact should be amplified in the presence of ventricular dilatation with attendant diastolic ventriculoannular disproportion [23]. Bot et al. validated that LV diastolic inflow volume and the size of the LV play a possible role in vortex ring formation [24]. Baccani et al. have also predicted in mathematical models that the presence of global LV dysfunction, such as in dilated cardiomyopathy; the LV filling vortex would result in increased intensity and longer stagnation near the apex [25]. A proposed useful physiological role of the vortex that cannot in fact aid ejection lies within its containing energy, which can assist reducing the pressure energy of the inflow [26]. Therefore, we deduced that more kinetic energy was trapped and dissipated in the ischemic failure LV in our study, and the large vortices accompanied with augmented ICV during whole early diastole should be a compensated appearance of the augmented filling pressure within the dilated failure LV cavity.

Furthermore, not like the IC limited to the basal level of LV cavity at baseline conditions, the IC appeared earlier at the LV middle and apical levels at T1, and was seen at each level of the LV cavity from T2 to T5 during cardiac ischemia in our study. As our wisdom, the IC and the ICV were determined by the intraventricular pressure gradients. Ling et al. reported 2–5 mmHg pressure difference between the mid-left ventricle and the apex in healthy dog LV during early diastole [27]. In addition, Courtois et al. observed in healthy dogs that a significant subbasal-apical early diastolic pressure gradient along the LV inflow tract with minimum pressure in the apex [14]. These results confirmed the active suction of the blood in left atrium toward the LV apex

under healthy conditions. Regional relaxation of the LV wall and the normal intraventricular pressure gradients should be damaged by myocardial ischemia [17], and the water-hammer effect of the LV inflow during early diastole must be enhanced by akinesis or dyskinesis of the regional ischemic LV wall.

We speculating that the significant changes of IC and the LV vortices in the acute ischemic failure LV cavity contrast to the baseline conditions were the direct reflection of the changes of LV intraventricular pressure fields, which accompanying with: (1) the damaged relaxation of the ischemic LV wall; (2) the dilated LV cavity and the possible changes of LV sharp and the inflow volume; (3) the changes of flow effect in LV fluid mechanics within the failure LV. In short, the characteristics of LV flow fields, such as the IC, embodies an extremely high sensitivity to the dynamic changes of LV boundary conditions, which always affected by cardiac ischemia. Therefore, intuitive visualization of IC and quantification of IC related index with VFM can provide preliminary support for developing of a new marker of heart healthy status.

Practical applications

The practical application of the described methods is that intuitive visualization IC and quantification of ICV within LV cavity on a three-dimensional flow plane with VFM is valuable for improving recognition of the subtle, flow-associated LV fluid dynamics in various physiological or pathophysiologic conditions. VFM may be a new and noninvasive diagnostic method of cardiac function based on ultrasonic visualization analysis of IC and quantification of IC related index.

Limitations

It is noteworthy that the IC described in our experiment is that of a complex circulation of LV blood cell in three-dimensional flow but only its special profiles were displayed. Although the conspicuous characteristics of LV flow fields during both baseline and ischemic conditions were reflected uniquely and sensitively, we could not correlate the IVC with the LV volumetric parameters and the invasively obtained pressure data successfully, and could not quantify and rank the heart function precisely with the ICV in this pilot study. We also stressed that while this is an "in vivo" model, in fact these hearts are exposed with relief of the pericardial constraint, and with catheters in the LV cavity. This may have undefined impacts, and limits the ability to extrapolate these findings to other situations where data is acquired noninvasively in un-instrumented hearts. Other limitation in our study is limited sample size, and the low spatio-temporal resolution of VFM as well as its limited velocity resolution of color Doppler flow imaging.

The characteristics of LV flow fields embodies an extremely high sensitivity to the boundary conditions such as the dynamic changes of LV geometry, the structure and function of mitral valves, the position of chordae and the musculi papillares, as well as other nonconservative force resulted from the heart rate, the relaxation of the LV myocardium, the cardiac twisting motion, and the changes of loading conditions [28]. We have to say that intuitive visualization and quantification of LV flow field provide no direct measure of myocardial mechanics, Therefore, the precise definition of the pathophysiological values of IC and the accurate relationship between the IC related index and the cardiac healthy status are real challenges for our further studies.

Conclusions

A highly valuable of VFM may be its use for visualization IC and quantification of ICV on profiles of LV flow fields, which can gives intriguing insights into normal and abnormal cardiac function through its intuitive visualization and quantification of the subtle, flow-associated LV fluid dynamics. As demonstrated in this study, ICV in LV cavity may be a new index of heart function. It will be of great practical importance to elucidate the physiological and pathophysiological significance of the IC and the accurate relationship between ICV and the cardiac healthy status in further studies, so as to determine whether the cardiac function can be precisely evaluated with IC related index, and to incorporate the VFM into clinical routine practice in the future.

Acknowledgments This work was supported by the National Nature Foundation of China (No. 30970698).

Conflict of interest None.

References

1. Richter Y, Edelman ER (2006) Cardiology is flow. Circulation 113:2679–2682
2. Kilner PJ, Yang GZ, Wilkes AJ, Mohiaddin RH, Firmin DN, Yacoub MH (2000) Asymmetric redirection of flow through the heart. Nature 404:759–761
3. De Mey S, De Sutter J, Vierendeels J, Verdonck P (2001) Diastolic filling and pressure imaging: taking advantage of the information in a colour M-mode Doppler image. Eur J Echocardiogr 2:219–233
4. Sengupta PP, Burke R, Khandheria BK, Belohlavek M (2008) Following the flow in chambers. Heart Fail Clin 4:325–332
5. Carlhäll CJ, Bolger A (2010) Passing strange: flow in the failing ventricle. Circ Heart Fail 3:326–331
6. Takatsuji H, Mikami T, Urasawa K, Teranishi J, Onozuka H, Takagi C, Makita Y, Matsuo H, Kusuoka H, Kitabatake A (1996) A new approach for evaluation of left ventricular diastolic function: spatial and temporal analysis of left ventricular filling flow propagation by color M-mode Doppler echocardiography. J Am Coll Cardiol 27:365–371
7. Stugaard M, Smiseth OA, Risöe C, Ihlen H (1993) Intraventricular early diastolic filling during acute myocardial ischemia, assessment by multigated color m-mode Doppler echocardiography. Circulation 88:2705–2713
8. Steine K, Stugaard M, Smiseth OA (1999) Mechanisms of retarded apical filling in acute ischemic left ventricular failure. Circulation 99:2048–2054
9. Ohtsuki S, Tanaka M (2006) The flow velocity distribution from the Doppler information on a plane in three-dimensional flow. J Vis 9:69–82
10. Uejima T, Koike A, Sawada H, Aizawa T, Ohtsuki S, Tanaka M, Furukawa T, Fraser AG (2010) A new echocardiographic method for identifying vortex flow in the left ventricle: numerical validation. Ultrasound Med Biol 36:772–788
11. Gharib M, Rambod E, Kheradvar A, Sahn DJ, Dabiri JO (2006) Optimal vortex formation as an index of cardiac health. Proc Natl Acad Sci USA 103:6305–6308
12. Ebbers T, Wigström L, Bolger AF, Wranne B, Karlsson M (2002) Noninvasive measurement of time-varying three-dimensional relative pressure fields within the human heart. J Biomech Eng 124:288–293
13. Jiamsripong P, Calleja AM, Alharthi MS, Dzsinich M, McMahon EM, Heys JJ, Milano M, Sengupta PP, Khandheria BK, Belohlavek M (2009) Impact of acute moderate elevation in left ventricular afterload on diastolic transmitral flow efficiency: analysis by vortex formation time. J Am Soc Echocardiogr 22:427–431
14. Courtois M, Kovács SJ Jr, Ludbrook PA (1988) Transmitral pressure-flow velocity relation. Importance of regional pressure gradients in the left ventricle during diastole. Circulation 78:661–671
15. Sabbah HN, Stein PD (1981) Pressure-diameter relations during early diastole in dogs. Incompatibility with the concept of passive left ventricular filling. Circ Res 48:357–365
16. Nakamura M, Wada S, Mikami T, Kitabatake A, Karino T (2003) Computational study on the evolution of an intraventricular vortical flow during early diastole for the interpretation of color M-mode Doppler echocardiograms. Biomech Model Mechanobiol 2:59–72
17. Beppu S, Izumi S, Miyatake K, Nagata S, Park YD, Sakakibara H, Nimura Y (1988) Abnormal blood pathways in left ventricular cavity in acute myocardial infarction. Experimental observations with special reference to regional wall motion abnormality and hemostasis. Circulation 78:157–164
18. Mohiaddin RH (1995) Flow patterns in the dilated ischemic left ventricle studied by MR imaging with velocity vector mapping. J Magn Reson Imaging 5:493–498
19. Taylor TW, Suga H, Goto Y, Okino H, Yamaguchi T (1996) The effects of cardiac infarction on realistic three-dimensional left ventricular blood ejection. J Biomech Eng 118:106–110
20. Delemarre BJ, Visser CA, Bot H, de Koning HJ, Dunning AJ (1989) Predictive value of pulsed Doppler echocardiography in acute myocardial infarction. J Am Soc Echocardiogr 2:102–109
21. Steine K, Stugaard M, Smiseth O (2002) Mechanisms of diastolic intraventricular regional pressure differences and flow in the inflow and outflow tracts. J Am Coll Cardiol 40:983–990
22. Duval-Moulin AM, Dupouy P, Brun P, Zhuang F, Pelle G, Perez Y, Teiger E, Castaigne A, Gueret P, Dubois-Randé JL (1997) Alteration of left ventricular diastolic function during coronary angioplasty-induced ischemia: a color M-mode Doppler study. J Am Coll Cardiol 29:1246–1255
23. Pasipoularides A, Shu M, Shah A, Womack MS, Glower DD (2003) Diastolic right ventricular filling vortex in normal and volume overload states. Am J Physiol Heart Circ Physiol 284:H1064–H1072
24. Bot H, Verburg J, Delemarre BJ, Strackee J (1990) Determinants of the occurrence of vortex rings in the left ventricle during diastole. J Biomech 23:607–615
25. Baccani B, Domenichini F, Pedrizzetti G, Tonti G (2002) Fluid dynamics of the left ventricular filling in dilated cardiomyopathy. J Biomech 35(5):665–671
26. Pierrakos O, Vlachos PP (2006) The effect of vortex formation on left ventricular filling and mitral valve efficiency. J Biomech Eng 128:527–539
27. Ling D, Rankin JS, Edwards CH II, McHale PA, Anderson RW (1979) Regional diastolic mechanics of the left ventricle in the conscious dog. Am J Physiol 236:H323–H330
28. Yang GZ, Merrifield R, Masood S, Kilner PJ (2007) Flow and myocardial interaction: an imaging perspective. Philos Trans R Soc Lond B Biol Sci 362:1329–1341